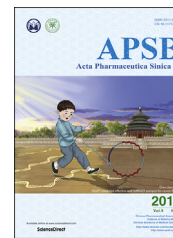




Chinese Pharmaceutical Association
Institute of Materia Medica, Chinese Academy of Medical Sciences

Acta Pharmaceutica Sinica B

www.elsevier.com/locate/apsb
www.sciencedirect.com



ORIGINAL ARTICLE

Silibinin ameliorates hepatic lipid accumulation and oxidative stress in mice with non-alcoholic steatohepatitis by regulating CFLAR-JNK pathway



Yayun Liu, Wei Xu, Ting Zhai, Jiaojiao You, Yong Chen*

Hubei Province Key Laboratory of Biotechnology of Chinese Traditional Medicine, National & Local Joint Engineering Research Center of High-throughput Drug Screening Technology, Hubei University, Wuhan 430062, China

Received 9 October 2018; received in revised form 11 December 2018; accepted 11 January 2019

KEY WORDS

Silibinin;
NASH;
CFLAR;
Lipid accumulation;
Oxidation stress

Abstract Non-alcoholic steatohepatitis (NASH) is a chronic metabolic syndrome and the CFLAR-JNK pathway can reverse the process of NASH. Although silibinin is used for the treatment of NASH in clinical, its effect on CFLAR-JNK pathway in NASH remains unclear. This study aimed to investigate the effect of silibinin on CFLAR-JNK pathway in NASH models both *in vivo* and *in vitro*. The *in vivo* study was performed using male C57BL/6 mice fed with methionine–choline-deficient diet and simultaneously treated with silibinin for 6 weeks. The *in vitro* study was performed by using mouse NCTC-1469 cells which were respectively pretreated with oleic acid plus palmitic acid, and adenovirus-down *Cflar* for 24 h, then treated with silibinin for 24 h. After the drug treatment, the key indicators involved in CFLAR-JNK pathway including hepatic injury, lipid metabolism and oxidative stress were determined. Silibinin

Abbreviations: *Acox*, acyl-coenzyme A oxidase X; Akt, serine–threonine protein kinase; ALT, alanine aminotransferase; AST, aspartate aminotransferase; CAT, catalase; CFLAR, caspase 8 and Fas-associated protein with death domain-like apoptosis regulator; *Cpt1a*, carnitine palmitoyl transferase 1 α ; CYP2E1, cytochrome P450 2E1; CYP4A, cytochrome P450 4A; *Fabp5*, fatty acid-binding proteins 5; *Gpat*, glycerol-3-phosphate acyltransferase; GSH-Px, glutathione peroxidase; HO-1, heme oxygenase 1; IR, insulin resistance; IRS1, insulin receptor substrate 1; JNK, c-Jun N-terminal kinase; HE, hematoxylin–eosin; MAPK, mitogen-activated protein kinase; MCD, methionine- and choline-deficient; MCS, methionine- and choline-sufficient; MT, Masson–Trichrome; NF- κ B, nuclear factor κ B; ORO, oil red O; MDA, malondialdehyde; *Mttp*, microsomal triglyceride transfer protein; NAFLD, non-alcoholic fatty liver disease; NASH, nonalcoholic steatohepatitis; NRF2, nuclear factor erythroid 2-related factor 2; OA, oleic acid; PA, palmitic acid; pIRS1, phosphorylation of insulin receptor substrate 1; PI3K, phosphatidylinositol 3-hydroxy kinase; pJNK, phosphorylation of c-Jun N-terminal kinase; *Pnpla3*, phospholipase domain containing 3; *Ppara*, peroxisome proliferator activated receptor α ; *Scd-1*, stearoyl-coenzyme A desaturase-1; SD, Sprague–Dawley; *Srebp-1c*, sterol regulatory element binding protein-1C; TC, total cholesterol; TG, triglyceride; 2-NBDG, 2-(*N*-(7-nitrobenz-2-oxa-1,3-diazol-4-yl) amino)-2-deoxyglucose

*Corresponding author. Tel./fax: +86 27 88663590.

E-mail address: cy101610@hubu.edu.cn (Yong Chen).

Peer review under responsibility of Institute of Materia Medica, Chinese Academy of Medical Sciences and Chinese Pharmaceutical Association.

<https://doi.org/10.1016/j.apsb.2019.02.006>

2211-3835 © 2019 Chinese Pharmaceutical Association and Institute of Materia Medica, Chinese Academy of Medical Sciences. Production and hosting by Elsevier B.V. This is an open access article under the CC BY-NC-ND license (<http://creativecommons.org/licenses/by-nc-nd/4.0/>).

significantly activated CFLAR and inhibited the phosphorylation of JNK, up-regulated the mRNA expression of *Ppara*, *Fabp5*, *Cpt1a*, *Acox*, *Scd-1*, *Gpat* and *Mttp*, reduced the activities of serum ALT and AST and the contents of hepatic TG, TC and MDA, increased the expression of NRF2 and the activities of CAT, GSH-Px and HO-1, and decreased the activities and expression of CYP2E1 and CYP4A *in vivo*. These effects were confirmed by the *in vitro* experiments. Silibinin prevented NASH by regulating CFLAR-JNK pathway, and thereby on one hand promoting the β -oxidation and efflux of fatty acids in liver to relieve lipid accumulation, and on the other hand inducing antioxidant activity (CAT, GSH-Px and HO-1) and inhibiting pro-oxidase activity (CYP2E1 and CYP4A) to relieve oxidative stress.

© 2019 Chinese Pharmaceutical Association and Institute of Materia Medica, Chinese Academy of Medical Sciences. Production and hosting by Elsevier B.V. This is an open access article under the CC BY-NC-ND license (<http://creativecommons.org/licenses/by-nc-nd/4.0/>).

1. Introduction

Non-alcoholic steatohepatitis (NASH) is a metabolic syndrome causing changes in the liver resembling those of alcoholic liver disease without a history of excessive drinking. These changes are characterized by excessive fatty degeneration in liver cells. The pathologic changes of NASH include simple fatty liver, fatty liver fibrosis, associated cirrhosis and liver cancer^{1–4}. NASH has the highest incidence among chronic liver diseases, and it may be the leading cause of liver transplantation in the next 10 years^{5,6}. The “two hit hypothesis” of NASH suggests that the excessive fat accumulation in the liver parenchyma is the first hit, which is related to drugs, diet, exercise and insulin resistance. The second hit is a cytotoxic reaction caused by the first hit, including oxidative stress and inflammatory responses⁷. As a chronic multi-system disease, NASH can also lead to many complications in other organs, such as chronic kidney disease, type 2 diabetes, cardiovascular and heart disease⁸.

Silibinin is a flavonolignan isolated from the fruit and seeds of Compositae Milk thistle. It has a wide range of pharmacological activities such as the functions of hepatoprotective, antioxidant, antineoplastic and maintaining the stability of liver cell membrane, and is reported to be the most effective flavonoid compound against hepatic disease^{9,10}. Silibinin can regulate insulin receptor substrate 1 (IRS-1)/phosphatidylinositol 3-hydroxy kinase (PI3K)/serine–threonine protein kinase (Akt) pathway to ameliorate dyslipidemia and insulin resistance in Sprague–Dawley (SD) rats fed by high-fat diet and in BRL3A and HepG2 cells pretreated by palmitic acid¹¹, inhibit nuclear factor κ B (NF- κ B) activity and improve hepatic nitrosative stress in *db/db* mice fed by methionine–choline deficiency (MCD) diet¹². It was reported that a silibinin–phospholipid complex prevented the mitochondrial dysfunction in Wistar rats fed by MCD diet¹³, and the mixture of silibinin, phosphatidylcholine and vitamin E was applied to treat patients with NASH in clinical¹⁴.

Caspase 8 and Fas-associated protein with death domain-like apoptosis regulator (CFLAR) can reverse the process of NASH¹⁵. Recent studies showed that CFLAR inhibited the phosphorylation of c-Jun N-terminal kinase (JNK), thereby ameliorated the pathological features of NASH, such as glucolipid metabolic disorder, oxidative stress, inflammation and liver fibrosis¹⁵. However, the effect of silibinin on CFLAR-JNK pathway related to NASH remains unclear. Given the important association between CFLAR-JNK pathway and the development of NASH, we investigated the effect of silibinin on CFLAR-JNK pathway and its downstream key genes involved in lipid metabolism and

oxidative stress in C57BL/6 mice fed with MCD diet and in NCTC-1469 cells (normal liver cell line of mice) pretreated with oleic acid (OA) and palmitic acid (PA)^{16,17}, and adenovirus-down *Cflar* in this paper. Our study will be beneficial for the further research of the preventive and therapeutic actions of silibinin and its structural analogues against NASH.

2. Materials and methods

2.1. Materials

C57BL/6 mice was obtained from Centers for Disease Prevention and Control of Hubei Province (Wuhan, China; the license number: SCXK 2011-0012). Methionine- and choline-sufficient (MCS) diet (Nantong Trophy Feed Technology Co. Ltd., Jiangsu, China) contains (per 1000 g): amino acid premix (methionine free) 175.7 g, methionine 8 g, choline chloride 2 g, sucrose 441.9 g, dextrin 50 g, corn starch 150.0 g, corn oil 100.0 g, cellulose 30.0 g, mineral mix 52.4 g. MCD diet (Nantong Trophy Feed Technology Co. Ltd.) contains (per 1000 g): amino acid premix (methionine free) 175.7 g, methionine 0 g, choline chloride 0 g, sucrose 431.9 g, dextrin 50 g, corn starch 150.0 g, corn oil 100.0 g, cellulose 30.0 g, mineral mix 52.4 g. Silibinin (HPLC \geq 98%) was from Shanghai Dingrui (Shanghai, China; CAS:32888-70-6). NCTC-1469 cells were provided by Hangzhou Haisheng Biotechnology Company (Hangzhou, China). Dulbecco's modified Eagle's medium (DMEM) and fetal bovine serum (FBS) were bought from Gibco (Carlsbad, CA, USA). Penicillin and streptomycin were from Hyclone (Hangzhou, China). Oleic acid (OA) was product of Aladdin (Shanghai, China). Palmitic acid (PA), 3-[4,5-dimethylthiazol-2-yl]-2,5-diphenyltetrazolium bromide (MTT), DMSO, and 12-hydroxylauric acid were product of Sigma (St. Louis, MO, USA). Cellular TG detection kit was provided from Applygen (Beijing, China). 2-(*N*-(7-Nitrobenz-2-oxa-1,3-diazol-4-yl) amino)-2-deoxyglucose (2-NBDG) and Trizol were from Invitrogen (Carlsbad, CA, USA). Glucose-free DMEM was from Hyclone (Logan, UT, USA). BCA kit was from Thermo (San Diego, CA, USA), Rever Tra Ace[®] qPCR RT kit from Toyobo (Shanghai, China), SYBR Green I fluorescent quantitative PCR kit from Bio-Rad (Hercules, CA, USA), kits for alanine aminotransferase (ALT) and aspartate aminotransferase (AST), total cholesterol (TC), triglyceride (TG), malondialdehyde (MDA), catalase (CAT), glutathione peroxidase (GSH-Px) and heme oxygenase 1 (HO-1) from Nanjing Jiancheng Biological Engineering Institute (Nanjing, China). Chlorzoxazone, 6-hydroxy chlorzoxazone, and 4'-hydroxytolbutamide were product

of TRC (Canada). Lauric acid was from Nu-Chek Prep (USA), and NADPH from BioFroxx (German). RIPA, PMSF, enhanced chemiluminescence liquid (ECL) were all products of Beyotime (Shanghai, China). Cocktail and phosphatase inhibitors were bought from Roche (Basel, Switzerland). PVDF membranes were products of Millipore (USA). Primary antibodies included polyclonal rabbit anti-mouse CFLAR, JNK, phosphorylation of JNK (p-JNK), insulin receptor substrate 1 (IRS1) and nuclear factor erythroid 2-related factor 2 (NRF2) were from Wanlei (Shenyang, China), phosphorylation of IRS1 (pIRS1) from Millipore (USA), CYP2E1 from Boster (Wuhan, China), CYP4A from Abcam (USA), and polyclonal mouse anti-mouse β -actin from Santa (USA). Secondary antibodies for CFLAR, JNK, p-JNK, IRS1, pIRS1, NRF2, CYP2E1 and CYP4A are horseradish peroxidase labeled goat anti-rabbit IgG (H+L) and for β -actin is horseradish peroxidase labeled goat anti mice IgG (H+L) (KPL, USA).

2.2. *In vivo* experiment

6–8 weeks male C57BL/6 mice were kept in a controlled environment ($22 \pm 2^\circ\text{C}$, $60 \pm 5\%$ relative humidity and 12/12 h day/dark cycle). Water and food were provided *ad libitum*. The handling of animals was approved by Ethics Committee for Scientific Research of Hubei University (Wuhan, China) and all experiments were performed in accordance with the institutional guidelines for the care and use of laboratory animals. Animals were randomly divided into 4 subgroups ($n = 8$): Group 1 was fed with for 6 weeks (MCS group); Group 2 was fed with MCD diet for 6 weeks (MCD group); Groups 3 and 4 were fed with MCD diet and administered simultaneously with silibinin by gavage at the respective dose of 10 and 20 mg/kg BW, once a day for 6 weeks. After the treatment mentioned above, mice were fasted for 12 h before being sacrificed. Body weight and liver weight were recorded. The serum was separated from the blood collected by extirpating the eyeballs. The liver was excised and perfused with saline. One portion of the liver from each mouse was fixed in 4% paraformaldehyde solution for histological analysis. One portion of the liver was used to prepare liver S9 fraction for the activity assay of cytochrome P450 2E1 (CYP2E1) and cytochrome P450 4A (CYP4A)¹⁸. One portion of the liver was used to prepare liver homogenate (liver-saline, 1:9, w/v) in ice water for the biochemical analysis. And one portion of the liver was frozen in liquid nitrogen for the detection of the mRNA and protein expression of target genes.

2.3. *In vitro* experiment

NCTC-1469 cells were cultured in DMEM supplemented with 10% FBS and 100 U/mL penicillin and 100 $\mu\text{g}/\text{mL}$ streptomycin at 37°C with 5% CO_2 and allowed to grow to 80% confluence.

In the *in vitro* experiment of NCTC-1469 cells pretreated by PA and OA, 1×10^6 cells were inoculated into each well of a 6-well plate. After cells adhered to the wells, they were divided into four groups: Group 1 was treated with cell culture medium (control group); Group 2 was pretreated with 0.25 mmol/L PA (dissolved in double distilled water) and 0.5 mmol/L OA (dissolved in methanol) at 37°C for 24 h (model group); Groups 3 and 4 were pretreated with PA and OA at 37°C for 24 h, and then treated with different concentrations (50 and 100 $\mu\text{mol}/\text{L}$) of silibinin (dissolved in DMSO) at 37°C for 24 h (silibinin groups).

In the *in vitro* experiment of NCTC-1469 cells transfected by adenovirus-mediated knock-down of *Cflar*, adenoviruses were prepared as previously described¹⁹. Short-hairpin RNA (shRNA)-encoding DNA sequences were synthesized and constructed into adenovirus plasmids by Haisheng Biological Technology Co. Ltd. (Shenzhen, China). The sequence of shRNA against *Cflar* were: F-5'-GGGAAGAGTGTCTTGATGAAGATTCAAGAGATCTTCATCAAGACACTCTTCCTTTTTTG-3', R-5'-GATCCAAAAAAGGAAGAGTGTCTTGATGAAGATCTTGAATCTTCATCAAGACACTCTTCCTGCA-3'. NCTC-1469 cells were inoculated into 6-well plate and divided into 4 groups: Group 1 was treated with adenoviruses expressing shRNA against luciferase (Ad-sh*Ctrl*) (control group); Group 2 was infected with adenovirus expressing shRNA against CFLAR (Ad-sh*Cflar*) at 100 plaque-forming units (PFU)/cell for 24 h (model group); Groups 3 and 4 were pretreated with Ad-sh*Cflar* for 24 h, and then treated with different concentrations of silibinin for 24 h (silibinin groups).

2.4. Cytotoxicity analysis

The cytotoxicity of silibinin on NCTC-1469 cells was measured by the MTT assay. Briefly, 1×10^3 cells were inoculated into each well of a 96-well plate. Cells were allowed to adhere to the wells and were then treated with different concentrations (0–200 $\mu\text{mol}/\text{L}$) of silibinin (dissolved in DMSO) at 37°C for 24 h. After addition of 20 μL of MTT (5 mg/mL) and 180 μL of PBS to each well for 4 h, the culture solution in the plate was removed and 150 μL of DMSO was added to each well to dissolve the formazan. Finally, the absorbance of each well was detected at 570 nm using a microplate reader (BIO-RAD). The amount of organic solvent in cell culture medium was consistent and controlled within 0.3%.

2.5. Cellular TG analysis

The content of TG in the tested cells was measured using a cellular TG detection kit according to the manufacturer's instruction after the treatment of PA and OA and silibinin (50 and 100 $\mu\text{mol}/\text{L}$) for 24 h in 6-well plates.

2.6. Glucose uptake analysis

The uptake 2-NBDG in NCTC-1469 cells were measured as follows: Cells inoculated in 6-well plate were co-treated with PA and OA for 24 h and then treated with silibinin (50 and 100 $\mu\text{mol}/\text{L}$) for 24 h, and finally were incubated in glucose-free DMEM with 50 $\mu\text{mol}/\text{L}$ 2-NBDG at 37°C for 30 min. The fluorescent intensity was measured using a multimode microplate reader (Berthold TriStar LB941, Germany) at excitation/emission wavelengths of 485 nm/535 nm. The protein concentration of each well was detected by BCA kit to normalize the data.

2.7. Real-time quantitative PCR

Total RNA was extracted from liver tissues using Trizol reagent and reverse transcribed to cDNA with Rever Tra Ace[®] qPCR RT kit as a template. SYBR Green I fluorescent quantitative PCR kit was used for the quantification of the mRNA expression of *Ppara*, *Fabp5*, *Cpt1a*, *Acox*, *Scd-1*, *Gpat*, *Mtp*, *Srebp-1c*, *Pnpla3*, *Cflar* and β -actin using the CFX Connect[™] real-time system (BIO-RAD). The primer sequences used for real-time quantitative PCR

Table 1 Primer sequences used for real-time quantitative PCR.

Gene	Primer	Sequence (5→3)
<i>β-Actin</i>	Forward	AACCGTGAAGATGACCCAGAT
	Reverse	CACAGCCTGGATGGCTACGTA
<i>Ppara</i>	Forward	CGGGAAAAGACCAGCAACAAC
	Reverse	ATAGCAGCCACAAACAGGGA
<i>Fabp5</i>	Forward	GGAAGGAGAGCACGATAACAAGA
	Reverse	GGTGGCATTGTTTCATGACACA
<i>Cpt1α</i>	Forward	TCCACCCTGAGGCATCTATT
	Reverse	ATGACCTCTGGCATTCTCC
<i>Acox</i>	Forward	CGGAAGATACATCCCGGAGACC
	Reverse	AAGTAGGACACCATAACCACC
<i>Scd-1</i>	Forward	TACTACAAGCCCGCCTCC
	Reverse	CAGCAGTACCAGGGCACCA
<i>Gpat</i>	Forward	CCATTGTGGAGGATGAAGTG
	Reverse	TGGATCGTGCCAGATAGGGA
<i>Mttp</i>	Forward	GCTAAGAAGCTGATAATGGGAGG
	Reverse	CCACTCTTGGAGAAACGGTCATA
<i>Srebp-1c</i>	Forward	TGGTAGACAACAGCCGCATC
	Reverse	CACTTCTGGAGACATCGCAAAC
<i>Pnpla3</i>	Forward	ATCCCTCTTCTCTGGCCTA
	Reverse	ATGTCATGCTACCGTAGAAAGG
<i>Cflar</i>	Forward	CTGTGTCTGCCGAGGTCATTC
	Reverse	AGAGCAATTCAGCCAAGGTAGC

Acox, acyl-coenzyme A oxidase X; *Cflar*, caspase 8 and Fas-associated protein with death domain-like apoptosis regulator; *Cpt1α*, carnitine palmitoyl transferase 1α; *Fabp5*, fatty acid-binding proteins 5; *Gpat*, glycerol-3-phosphate acyltransferase; *Mttp*, microsomal triglyceride transfer protein; *Pnpla3*, phospholipase domain containing 3; *Ppara*, peroxisome proliferator activated receptor α; *Scd-1*, stearoyl-coenzyme A desaturase-1; *Srebp-1c*, sterol regulatory element binding protein-1C.

were shown in Table 1. RT-qPCR were performed for 40 cycles at the following conditions: pre-denaturation at 95 °C for 5 min, denaturation at 95 °C for 30 s, annealing at 58.3 °C for 30 s, extended at 72 °C for 30 s. The expression of target genes was normalized to that of *β-actin*, and the relative quantification of mRNA levels was performed using the $2^{-\Delta\Delta Ct}$ method.

2.8. Histological analysis

Hepatic steatosis, inflammation and fibrosis were assessed by hematoxylin–eosin (HE), oil red O (ORO), and Masson–Trichrome (MT) staining as described in Flores-Costa et al.²⁰

2.9. Biochemical analysis

The levels of ALT and AST in serum, as well as TC, TG, MDA, CAT, GSH-Px and HO-1 in liver homogenate were determined by standard laboratory detection kits according to the manufacturer's instructions.

2.10. Determination of hepatic CYP2E1 and CYP4A activities

The activities of CYP2E1 and CYP4A in liver S9 fractions were determined by an LC–MS/MS system consisting of LC-20AD parallel pump, SIL-20A autosampler, DGU-20A3R degasser unit, CTO-20A column oven, and MS-8040 spectrometer (Shimadzu, Japan). The probe substrate was chlorzoxazone for CYP2E1 and lauric acid for CYP4A. The activities of CYP2E1 and CYP4A were calculated according to the production of 6-hydroxy chlorzoxazone and 12-hydroxylauric acid in the incubation system. Incubation was performed at 37 °C for 20 min in 200 μL of potassium phosphate buffer (0.1 mol/L, pH 7.4) including 50 μmol/L chlorzoxazone, 0.6 mg/mL liver S9, 5 mmol/L MgCl₂ and 1 mmol/L NADPH for CYP2E1, 100 μmol/L lauric acid, 0.5 mg/mL liver S9, 5 mmol/L MgCl₂ and 1 mmol/L NADPH for CYP4A. After incubation, 800 μL of cold ethyl acetate containing internal standard 4'-hydroxytolbutamide (0.08 μmol/L for CYP2E1 and 0.72 μmol/L for CYP4A) was added to stop the reaction. The supernatant was collected after centrifugation (12,000 × g for 10 min) at 4 °C, and evaporated to dryness at 30 °C. The residue was dissolved in 100 μL mobile phase (acetonitrile:H₂O, 1:1, v/v) to detect the concentration of 6-hydroxy chlorzoxazone and 12-hydroxylauric acid. 6-Hydroxy chlorzoxazone was separated on Shim-pack ODS C18 column (150 mm × 2.0 mm, 4.6 μm) using the mobile phase of mixed water (containing 0.1% formic acid) (A)/acetonitrile (B) at gradient elution program (0–5 min, 30%–85% B; 5–6 min, 85% B; 6–6.01 min, 85%–30%B; 6.01–11 min, 30% B; a flow rate of 0.2 mL/min), and detected by negative ion multiple reaction monitoring with *m/z* 184.0→120.1 for 6-hydroxy chlorzoxazone and 285.0→186.1 for IS. 12-Hydroxylauric acid was separated on the above stated column and the mobile phase by gradient elution (0–4 min, 25%–90% B; 4–8 min, 90% B; 8–8.01 min, 90%–25% B, 8.01–13 min, 25% B; a flow rate of 0.3 mL/min), and detected by negative ion selective ion monitoring with *m/z* 215.0 for 12-hydroxylauric acid and 184.0 for IS. The column temperature was 40 °C.

2.11. Western blot

Total protein lysates of mouse liver tissues and NCTC-1469 cells were obtained by incubation on ice with RIPA containing 1% PMSF, cocktail and phosphatase inhibitors. The supernatant was collected after centrifugation at 12,000 × g for 15 min at 4 °C. Protein quantification was performed with a BCA kit. Aliquots containing 30 μg of protein were separated by SDS-PAGE (5% concentrated gel and 10% separated gel) and transferred to PVDF membranes. The membrane was incubated with 5% nonfat dried milk at room temperature for 2 h, followed by specific primary antibodies at 4 °C overnight and the corresponding secondary antibodies at room temperature for 1 h. Immunoreactive bands were visualized by ECL and quantified by software Image J (NIH, USA).

2.12. Statistical analysis

Results were presented as the mean ± standard deviation (SD), $n = 8$. Statistical analyses were performed using one-way analysis of variance (ANOVA), followed by Tukey's test. Values were considered significant at $P < 0.05$.

3. Results

3.1. In vivo effects of silibinin on hepatic index and histological changes

The changes in the body weight, the liver weight and the hepatic index (liver weight/body weight × 100) after the six-week treatments were shown in Fig. 1. The body weight, the liver weight and the hepatic index of MCD group was significantly lower than MCS group. Silibinin treatment increased the hepatic index, especially with the high dose of silibinin (20 mg/kg), the liver index returned to the level of MCS group. The results indicated that feeding MCD diet decreased the hepatic index of mice, whereas exposure to silibinin prevented the decrease of hepatic index of mice induced by feeding MCD diet.

The liver histological changes of the tested mice including hepatic steatosis, ballooning, inflammation and fibrosis were shown in Fig. 2. The results from HE and ORO staining showed the intracellular steatosis, ballooning and inflammation in MCD group as compared

with MCS group, whereas the histological changes induced by feeding MCD diet were restored by silibinin treatment. In addition, no significant differences in hepatic fibrosis was observed in the 4 experimental groups based on the results of MT staining.

3.2. In vivo effects of silibinin on biomarkers of hepatic injury

The levels of serum ALT and AST, and hepatic TC, TG and MDA were shown in Table 2. The activities of ALT and AST in serum, and the contents of TC, TG and MDA in liver homogenate were significantly higher in MCD group than MCS group. These results indicated that MCD diet led to liver injury and fat accumulation of mice. Compared to MCD group, silibinin treatment decreased the levels of ALT, AST, TC, TG and MDA. However, in addition to TC and TG, the levels of ALT, AST and MDA in silibinin groups were not back to normal as compared with MCS group. These results showed that silibinin treatment had a beneficial effect on liver injury and fat accumulation induced by feeding MCD diet.

3.3. In vivo effects of silibinin on the activities of hepatic oxidative stress-related enzymes

The effects of silibinin on the activities of oxidative stress-related enzymes including the family of oxygen radical

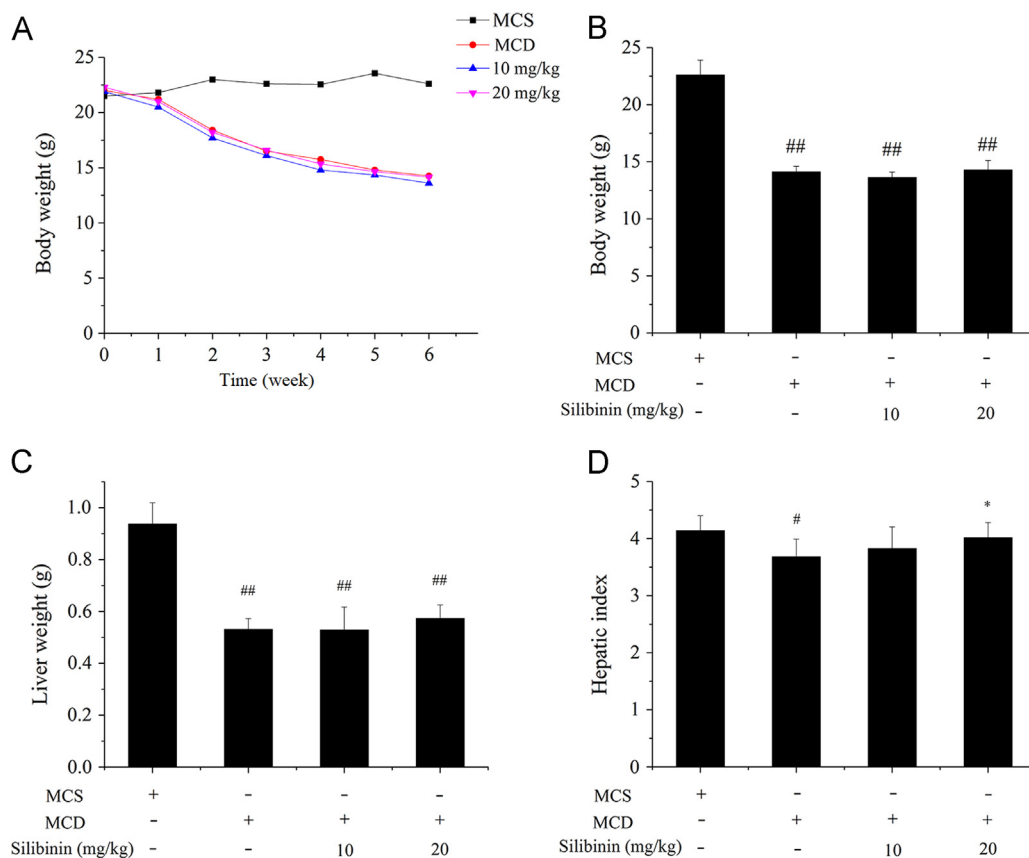


Figure 1 Effects of silibinin on body weight, liver weight and hepatic index in different groups of mice. C57BL/6 were treated with MCD and silibinin for 6 weeks and the body weight during 6 weeks (A), the body weight (B), liver weight (C) and hepatic index (D) after 6 weeks in different groups of mice were detected. Values (mean ± SD) were obtained from each group ($n = 8$) after 6 weeks of the experimental period. # $P < 0.05$ and ## $P < 0.01$ versus MCS group; * $P < 0.05$ and ** $P < 0.01$ versus MCD group. MCD, methionine- and choline-deficient; MCS, methionine- and choline-sufficient.

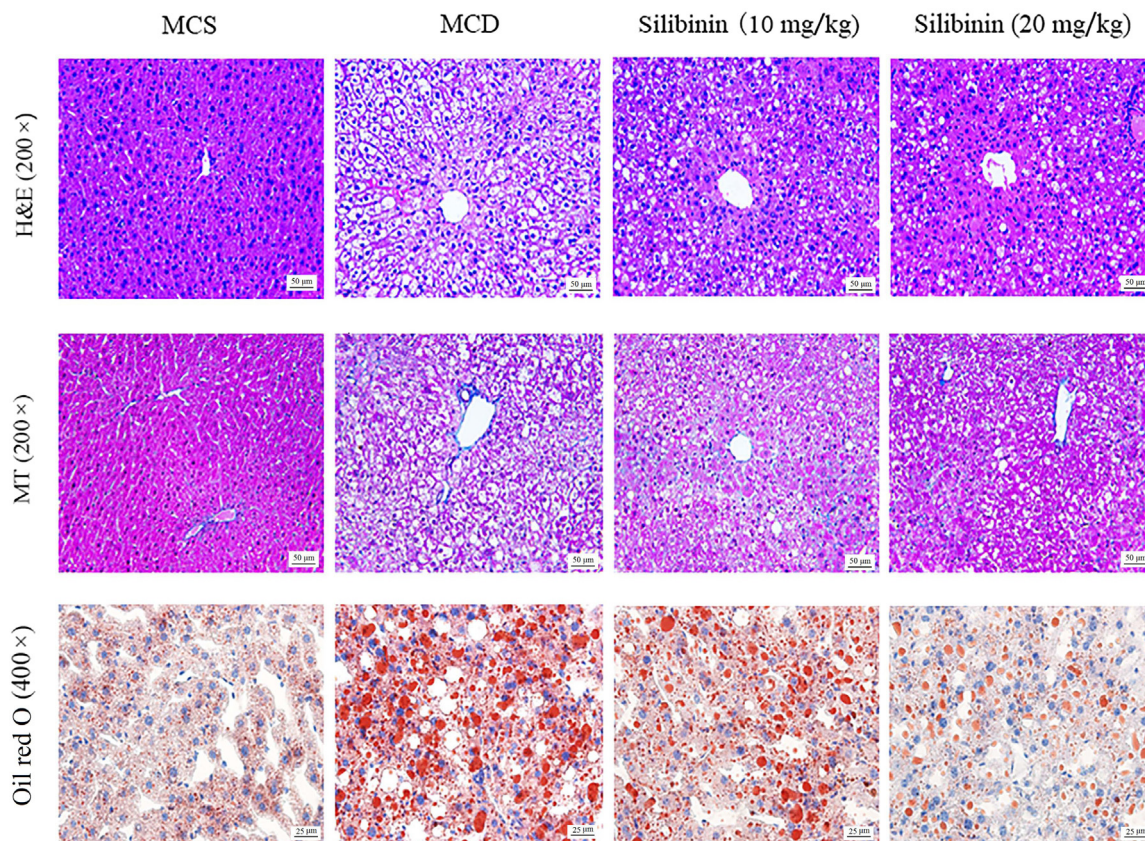


Figure 2 Effects of silibinin on hepatic histological changes. H&E, MT and oil red O staining of liver sections in different groups of mice. HE, hematoxylin and eosin; MCD, methionine- and choline-deficient; MCS, methionine- and choline-sufficient; MT, Masson–Trichrome.

Table 2 Effect of silibinin on biomarkers of hepatic injury in C57BL/6 mice.

Biomarker	MCS	MCD	Silibinin (mg/kg)	
			10	20
Serum ALT (U/L)	8.58 ± 1.13	41.42 ± 9.38 ^{##}	31.11 ± 8.78 ^{###**}	26.81 ± 10.00 ^{###**}
Serum AST (U/L)	21.37 ± 3.98	40.32 ± 6.23 ^{##}	39.19 ± 9.71 ^{##}	31.46 ± 6.80 ^{##*}
Hepatic TC (mmol/gprot)	0.09 ± 0.01	0.17 ± 0.04 ^{##}	0.09 ± 0.01 ^{**}	0.05 ± 0.02 ^{##**}
Hepatic TG (mmol/gprot)	0.14 ± 0.03	0.35 ± 0.03 ^{##}	0.22 ± 0.035 ^{**}	0.19 ± 0.01 ^{**}
Hepatic MDA (nmol/mgprot)	0.91 ± 0.24	6.15 ± 1.48 ^{##}	5.62 ± 1.73 ^{##}	2.34 ± 0.44 ^{#**}

Values (mean ± SD) were obtained from each group ($n = 8$) after 6 weeks of the experimental period. [#] $P < 0.05$ and ^{##} $P < 0.01$ versus MCS group; ^{*} $P < 0.05$ and ^{**} $P < 0.01$ versus MCD group. ALT, alanine aminotransferase; AST, aspartate aminotransferase; MDA, malondialdehyde; MCD, methionine- and choline-deficient; MCS, methionine- and choline-sufficient; TC, total cholesterol; TG, triglyceride.

scavenging enzymes (CAT, GSH-Px and HO-1) and oxygen free radical generating enzymes (CYP2E1 and CYP4A) were shown in Table 3. Compared with MCS group, the activities of CAT, GSH-Px and HO-1 in MCD group were significantly decreased, whereas the activities of CYP2E1 and CYP4A in MCD group were significantly increased. Compared with MCD group, silibinin treatment increased the activities of CAT, GSH-Px and HO-1. It also suppressed the activities of CYP2E1 and CYP4A. More importantly, silibinin treatment almost restored the enzymatic activity mentioned above to normal.

3.4. In vivo effects of silibinin on the mRNA expression of hepatic lipid accumulation-related genes

The effects of silibinin on the mRNA expression of hepatic lipid synthesis related genes (*Srebp-1c* and *Pnpla3*), lipid oxidation related genes (*Ppara*, *Fabp5*, *Cpt1a* and *Acox*) and fatty acid transport related genes (*Gpat*, *Mttp* and *Scd-1*) were shown in Fig. 3. Compared with MCS group, the mRNA expression of *Ppara*, *Fabp5*, *Cpt1a*, *Acox*, *Scd-1*, *Gpat* and *Mttp* were significantly lower in the MCD group. Silibinin treatment increased the mRNA levels of *Ppara*, *Fabp5*, *Cpt1a*, *Acox*, *Scd-1*, *Gpat* and

Table 3 Effect of silibinin on activities of hepatic antioxidant enzymes in C57BL/6 mice.

Hepatic enzyme	MCS	MCD	Silibinin (mg/kg)	
			10	20
CAT (U/mgprot)	22.56 ± 2.42	8.98 ± 1.22 ^{###}	17.69 ± 3.54 ^{**}	21.09 ± 4.13 ^{**}
GSH-Px (U/mgprot)	324.39 ± 42.04	189.57 ± 23.68 ^{###}	268.54 ± 34.89 ^{**}	272.47 ± 43.11 ^{**}
HO-1 (ng/mgprot)	3.42 ± 0.41	1.13 ± 0.19 ^{###}	1.59 ± 0.22 ^{###*}	2.17 ± 0.3 ^{#**}
CYP2E1 (nmol/mgprot min)	0.19 ± 0.04	0.31 ± 0.04 ^{###}	0.24 ± 0.06 [*]	0.23 ± 0.03 ^{**}
CYP4A (nmol/mgprot min)	0.16 ± 0.03	0.24 ± 0.03 ^{###}	0.19 ± 0.07	0.17 ± 0.01 ^{**}

Values (mean ± SD) were obtained from each group ($n = 8$) after 6 weeks of the experimental period. [#] $P < 0.05$ and ^{###} $P < 0.01$ versus MCS group; ^{*} $P < 0.05$ and ^{**} $P < 0.01$ versus MCD group. CAT, catalase; CYP2E1, cytochrome P450 2E1; CYP4A, cytochrome P450 4A; GSH-Px, glutathione peroxidase; HO-1, heme oxygenase 1; MCD, methionine- and choline-deficient; MCS, methionine- and choline-sufficient.

Mtp, although the mRNA expression levels of the tested genes were significantly lower than those of MCS group. No significant difference was observed for the mRNA expression of *Srebp-1c* and *Pnpla3* among MCS, MCD and silibinin groups.

3.5. In vivo effects of silibinin on the protein expression of hepatic CFLAR-JNK pathway-related genes

The protein expression levels of hepatic CFLAR-JNK pathway-related genes including CFLAR, pJNK, NRF2, CYP2E1 and CYP4A in the 4 groups of mice were shown in Fig. 4. Compared to MCS group, the protein expression levels of CFLAR and NRF2 in MCD group were significantly decreased. The protein expression levels of pJNK/JNK, CYP2E1 and CYP4A in MCD group were significantly increased. Silibinin treatment increased the protein expression levels of CFLAR and NRF2, whereas reduced the protein expression levels of pJNK/JNK, CYP2E1 and CYP4A. In addition, silibinin treatment restored the protein expression of CFLAR and pJNK/JNK to the normal level while the protein expression of NRF2, CYP2E1 and CYP4A could not be returned to normal.

3.6. In vitro effects of silibinin on the contents of intracellular TG and 2-NBDG, and the expression of CFLAR-JNK pathway-related genes in OA and PA pretreated NCTC-1469 cells

The effects of silibinin (0, 5, 10, 20, 50, 100 and 200 $\mu\text{mol/L}$) on the viability of NCTC-1469 cells at 24, 48 and 72 h were shown in Fig. 5A. Except 100 $\mu\text{mol/L}$ silibinin treatment for 72 h and 200 $\mu\text{mol/L}$ treatment for 48 and 72 h, other cases of silibinin treatment had no significantly effect on the viability of NCTC-1469 cells. Therefore, 50 and 100 $\mu\text{mol/L}$ silibinin were chosen to treat NCTC-1469 cells for 24 h in subsequent experiments.

Fig. 5B and C showed the effect of silibinin on TG content and the ORO staining in OA- and PA-pretreated NCTC-1469 cells. The content of TG in model group was 8.6 times higher than that of control group. Treatment with 50 and 100 $\mu\text{mol/L}$ silibinin decreased TG content to 80% and 71% of model group, respectively. The results of ORO staining were consistent with TG.

Fig. 5D showed the effect of silibinin on the uptake of 2-NBDG in OA and PA pretreated NCTC-1469 cells. OA and PA pretreatment repressed the uptake of 2-NBDG in cells and silibinin treatment for 24 h relieved the inhibiting effect.

The effects of silibinin treatment on CFLAR, pJNK, NRF2 and pIRS1 protein expression in OA and PA pretreated NCTC-1469 cells were shown in Fig. 5E–I. OA and PA pretreatment down-

regulated the protein expression of CFLAR, NRF2 and pIRS1 and up-regulated the protein expression of pJNK in model group, whereas silibinin treatment for 24 h up-regulated the expression of CFLAR, NRF2 and pIRS1 and down-regulated the expression of pJNK in a dose-dependent manner.

3.7. In vitro effect of silibinin on the expression of CFLAR-JNK pathway-related genes in NCTC-1469 cells transfected with Ad-shCflar

The effect of silibinin treatment for 24 h on the expression of CFLAR downstream signaling molecules in NCTC-1469 cells transfected with Ad-shCflar were investigated and the results were shown in Fig. 6. Ad-shCflar treatment for 24 h inhibited the mRNA and protein expression of CFLAR, promoted the phosphorylation of JNK and restrained the protein expression of NRF2 and pIRS1. Silibinin treatment for 24 h up-regulated the mRNA expression of *Cflar* and the protein expression of CFLAR, NRF2 and pIRS1, while down-regulated the protein expression of pJNK in a dose-dependent manner.

4. Discussion

Epidemiological studies show that changes in lifestyle and increased fat in daily diet have increased the incidence of obesity, hyperlipidemia and diabetes, thus significantly increased the risk of NASH. While the morbidity rate of NASH in different countries is approximately 10%–24%, in obese population it is much higher, approximately 57%–74%²¹. Day et al.²² reported that 15%–50% of patients have hepatic fibrosis, 7%–25% have cirrhosis, and the survival rate at 5 and 10 years is 67% and 59% in NASH patients, respectively. Therefore, the study of the pathogenesis, prevention and treatment of NASH is a research hot spot. In this paper, we studied the effects and mechanism of action of silibinin on lipid metabolism and oxidative stress in NASH models including C57BL/6 mice fed with MCD diet and NCTC1469 cells treated with PA and OA and adenovirus-mediated knock-down of *Cflar*.

CFLAR is a member of the innate immune regulatory network. It modulates apoptosis through mitogen-activated protein kinase (MAPK)/JNK pathway in liver cells²³, inhibits JNK pathway to improve the activity of immune cells and attenuate the symptoms of diabetic rats induced by streptozocin²⁴. Glucolipid metabolism, inflammatory responses, insulin resistance, fibrosis and oxidative stress disorder were significantly enhanced in *Cflar*-knockout mice, whereas CFLAR overexpression mice showed a significant improvement or even reversal of these pathological features^{15,25}. The effect of

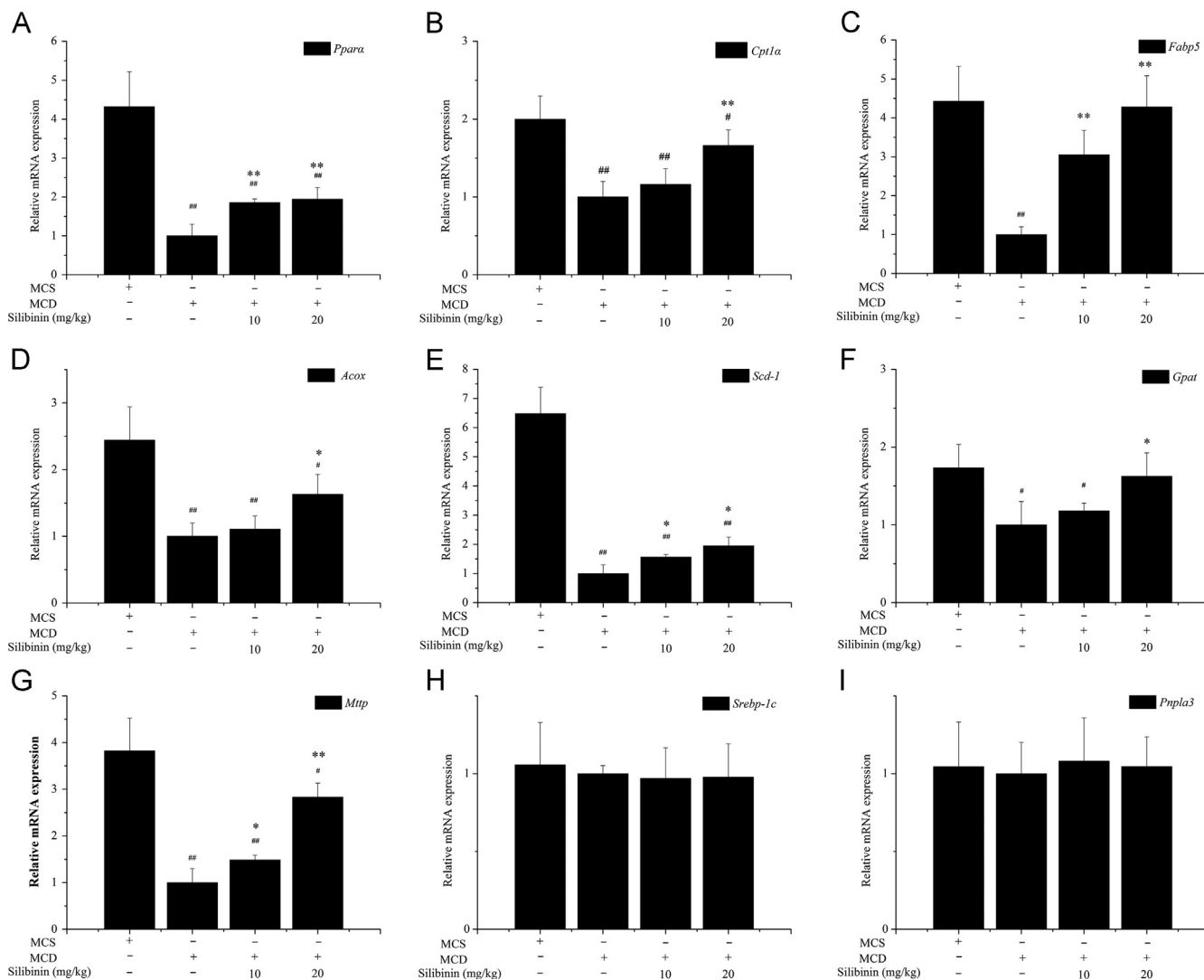


Figure 3 Effects of silibinin on the mRNA expression of hepatic lipid accumulation-related genes in different groups of mice. Values (mean \pm SD) were obtained from each group ($n = 8$) after 6 weeks of the experimental period. # $P < 0.05$ and ## $P < 0.01$ versus MCS group; * $P < 0.05$ and ** $P < 0.01$ versus MCD group. *Acox*, Acyl-coenzyme A oxidase X; *Cflar*, caspase 8 and Fas-associated protein with death domain-like apoptosis regulator; *Cpt1a*, carnitine palmitoyl transferase 1 α ; *Fabp5*, fatty acid-binding proteins 5; *Gpat*, glycerol-3-phosphate acyltransferase; MCD, methionine- and choline-deficient; MCS, methionine- and choline-sufficient; *Mtp*, microsomal triglyceride transfer protein; *Pnpla3*, phospholipase domain containing 3; *Ppara*, peroxisome proliferator activated receptor α ; *Scd-1*, stearoyl-coenzyme A desaturase-1; *Srebp-1c*, sterol regulatory element binding protein-1C.

silibinin on CFLAR expression observed in our study are consistent with the literature reports¹⁵, indicating that silibinin can activate CFLAR and inhibit the expression of its downstream pJNK/JNK *in vivo* and *in vitro*. In order to further clarify the mechanism of silibinin to NASH, we focused on the silibinin-induced effects on the expression of downstream target genes of JNK involved in lipid metabolism, oxidative stress and insulin resistance.

Lipid accumulation in the liver is mainly related to the expression of lipid synthesis genes (such as *Srebp-1c* and *Pnpla3*), lipid oxidative genes (such as *Ppara*, *Fabp5*, *Cpt1a* and *Acox*) and lipid transport genes (such as *Scd-1*, *Gpat* and *Mtp*). *Ppara*, *Fabp5*, *Cpt1a* and *Acox* are key genes involved in lipid acid β -oxidation. *Ppara* belongs to the type II nuclear receptors and its expression was significantly down-regulated in the liver of MCD diet feeding-induced NASH mouse model²⁶. *Ppar* agonists might play a role in rat with NASH by triggering enzyme activities

related to lipid metabolism (e.g., *Fabp*, *Cpt* and *Acox*)²⁷, and drugs targeting *PPAR α* were used for the clinical treatment of dyslipidemia²⁸. CPT1 and ACOX are key limiting enzymes of fatty acid β -oxidation that are regulated by *PPAR α* ²⁹. FABP5 is a necessary condition for the use of long chain fatty acids by the liver³⁰. Our results showed that the mRNA expression of *Ppara*, *Fabp5*, *Cpt1a* and *Acox* in MCD group were significantly inhibited, and silibinin had an antagonistic effect on the inhibition induced by feeding MCD diet, indicating that silibinin could promote hepatic fatty acid β -oxidation. *Scd-1*, *Gpat* and *Mtp* are related to the transport of fatty acids out of the liver^{31–33}, the expression of them in NASH model were significantly inhibited^{34–36}. The lack of *Mtp* directly led to fatty liver disease and cirrhosis³⁷. Our results showed that the mRNA expression of *Scd-1*, *Gpat* and *Mtp* were significantly inhibited in MCD group, and silibinin could alleviate MCD diet-induced inhibitory effect, indicating that silibinin could promote

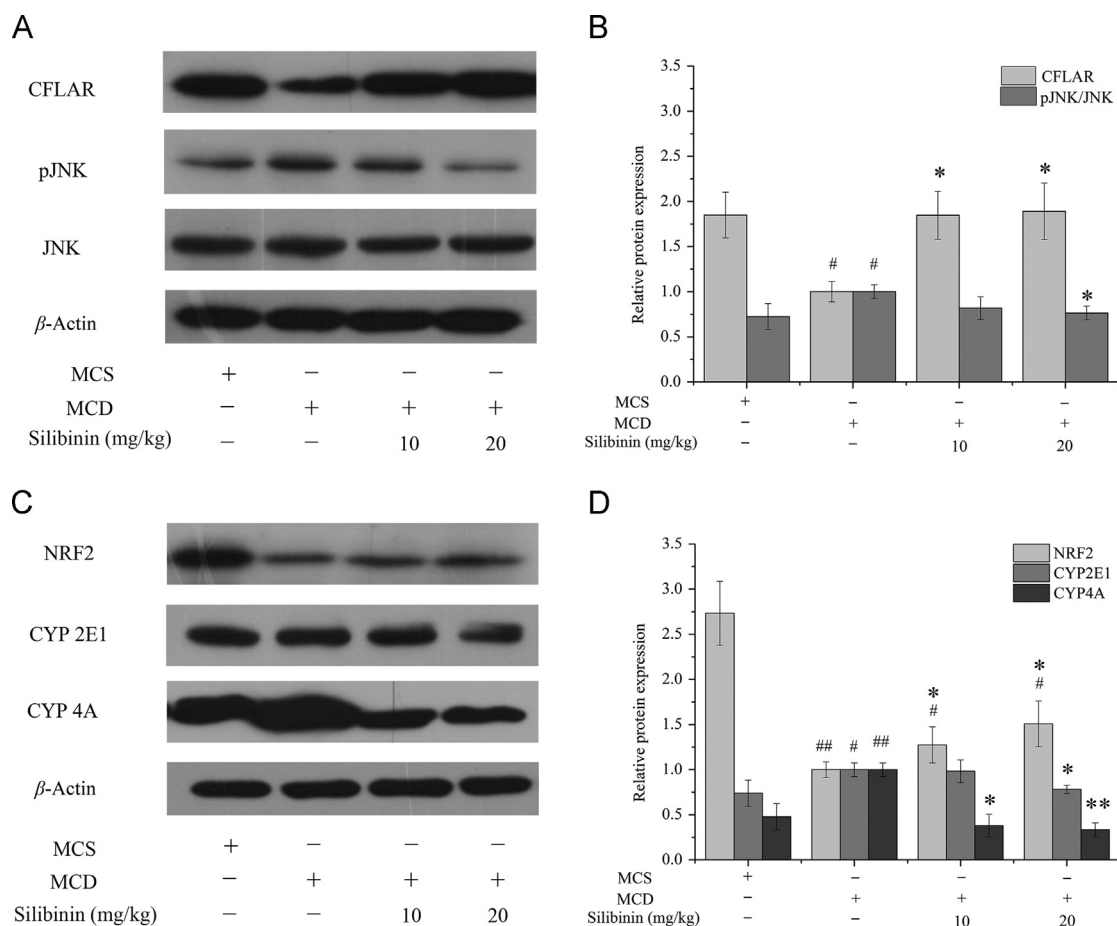


Figure 4 Effects of silibinin on the protein expression of hepatic CFLAR-JNK pathway related genes in different groups of mice. Values (mean \pm SD) were obtained from each group ($n = 8$) after 6 weeks of the experimental period. $\#P < 0.05$ and $\###P < 0.01$ versus MCS group; $*P < 0.05$ and $**P < 0.01$ versus MCD group. CFLAR, caspase 8 and Fas-associated protein with death domain-like apoptosis regulator; JNK, c-Jun N-terminal kinase; MCD, methionine- and choline-deficient; MCS, methionine- and choline-sufficient; NRF2, nuclear factor erythroid 2-related factor 2; pJNK, phosphorylation of c-Jun N-terminal kinase.

the transfer of fatty acids out of the liver. MCD diet and silibinin had no significant effect on the mRNA expression of lipid synthesis-related genes in the liver. Additionally, we found that silibinin treatment reduced the levels of hepatic TG and TC in C57BL/6 mice fed by MCD diet, as well as TG content in NCTC-1469 cells pretreated by PA and OA. These results indicated that silibinin alleviated the hepatic fat accumulation of NASH by promoting hepatic lipid oxidation and fatty acid transport out of the liver to the first hit in NASH.

Insulin resistance (IR) is closely related to the first hit of NASH and can promote the development of the disease course of NASH. IR causes hyperinsulinemia and promotes the fat decomposition in peripheral tissues which would increase the free fatty acids in blood and liver. At the same time, large amounts of free fatty acids will generate triglycerides in the liver because of the oxidation disorder^{38,39}. IR can inhibit glucose uptake in cells^{40–42} and can be improved by phosphorylation of IRS1 downstream of JNK⁴³. Our results showed that silibinin could meliorate the IR by promoting the phosphorylation of IRS1 in NCTC-1469 cells.

Oxidative stress is a state when the antioxidant enzyme systems are inhibited, and pro-oxidative reactions are activated. The excess free radicals in the body lead to DNA oxidative damage and abnormal expression of various proteins related to cytotoxicity, which is closely related to the development of NAFLD and observed in

almost all patients with NAFLD⁴⁴. In the present work, we examined the effect of silibinin on hepatic oxidative stress from two aspects including scavenging and production of reactive oxygen. NRF2 is a highly sensitive transcription factor related to oxidative stress and plays a key role in the expression of a variety of antioxidant genes and phase II detoxification enzymes^{45–48}. The expression of NRF2 is significantly inhibited in MCD diet-induced NASH model, whereas activation of NRF2 significantly improves various symptoms of NASH⁴⁹. CAT, GSH-Px and HO-1 are important enzymes for scavenging free radicals in organisms, which can alleviate lipid peroxidation of cell membranes^{50,51}. CYP2E1 and CYP4A are important enzymes for the generation of free radicals in the body, and also are important factors inducing fatty liver disease in wild-type mice⁵², the activity and expression of them are increased in patients and rodents with fatty liver and positively related to lipid peroxidation levels^{53–55}. Our results showed that the protein expression of NRF2 *in vivo* and *in vitro*, as well as the activities of anti-oxidative enzymes including CAT, GSH-Px and HO-1 *in vivo*, were all upregulated, and the enzyme activity and protein expression of CYP2E1 and CYP4A were repressed in the liver of mice with NASH following silibinin treatment. The results indicated that silibinin could improve NASH-related oxidative stress injury by increasing the antioxidase activity and inhibiting the activities of free radical generating enzymes in the liver.

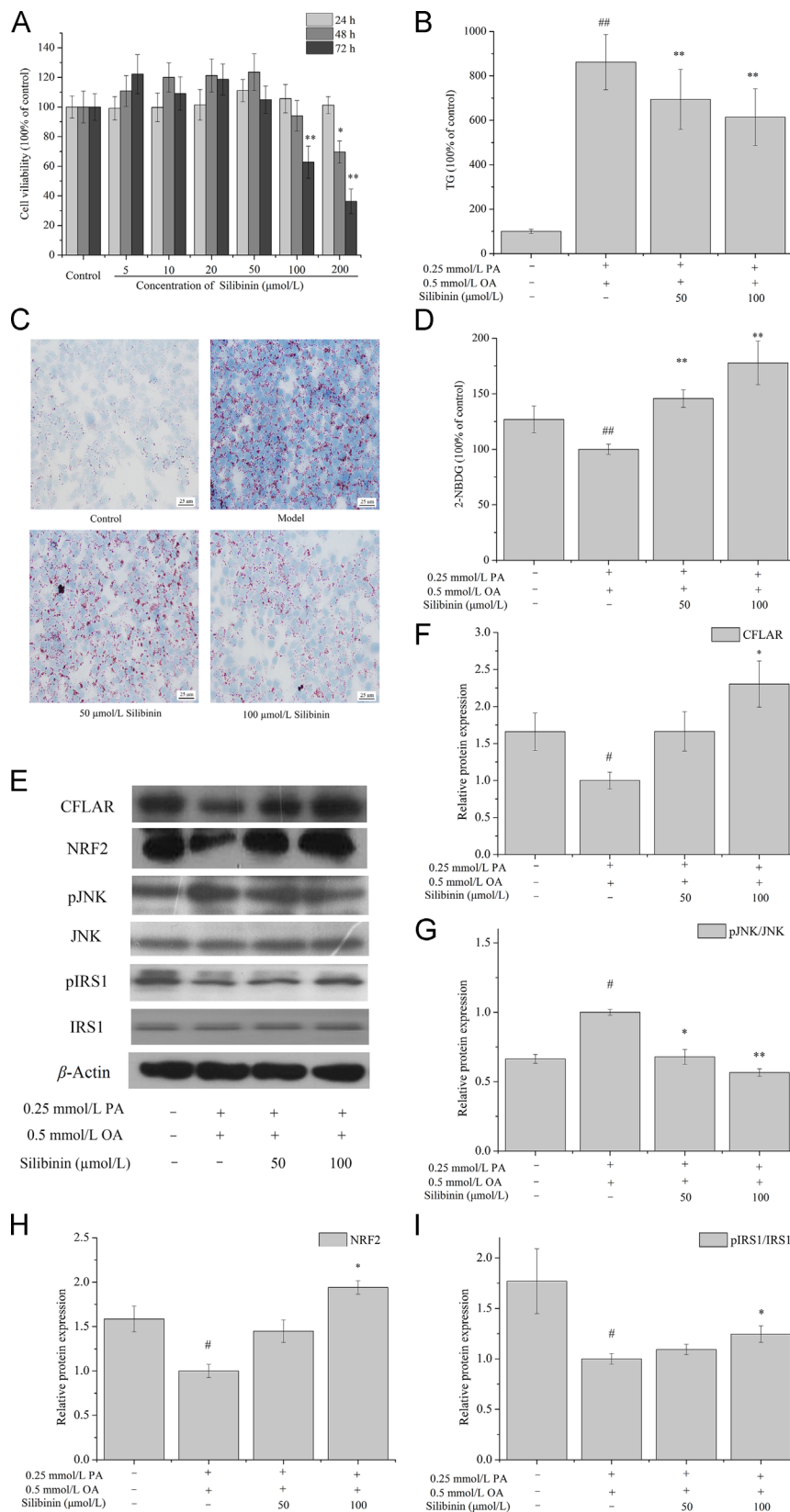


Figure 5 Effects of silibinin on cellular TG and 2-NBDG contents, and the protein expression of CFLAR, pJNK/JNK, NRF2 and pIRS1/IRS1 in OA and PA pretreated NCTC-1469 cells. NCTC-1469 cells were pretreated with OA and PA and then treated with silibinin to detect the cellular viability (A), TG (B), oil red O staining (C), 2-NBDG (D), protein expression of CFLAR, NRF2, pJNK/JNK and pIRS1/IRS1 (E)–(I). The representative results from three independent experiments were shown. Cellular protein expression levels were analyzed by Western blot. The relative protein levels were determined after normalization with β -actin. The data were expressed as the means \pm SD. $\#P < 0.05$ and $\#\#P < 0.01$ versus control group; $*P < 0.05$ and $**P < 0.01$ versus model group. Scale bar=25 μ m. CFLAR, caspase 8 and Fas-associated protein with death domain-like apoptosis regulator; IRS1, insulin receptor substrate 1; JNK, c-Jun N-terminal kinase; NRF2, nuclear factor erythroid 2-related factor 2; OA, oleic acid; PA, palmitic acid; pIRS1, phosphorylation of insulin receptor substrate 1; pJNK, phosphorylation of c-Jun N-terminal kinase; TG, triglyceride; 2-NBDG, 2-(N-(7-nitrobenz-2-oxa-1,3-diazol-4-yl) amino)-2-deoxyglucose.

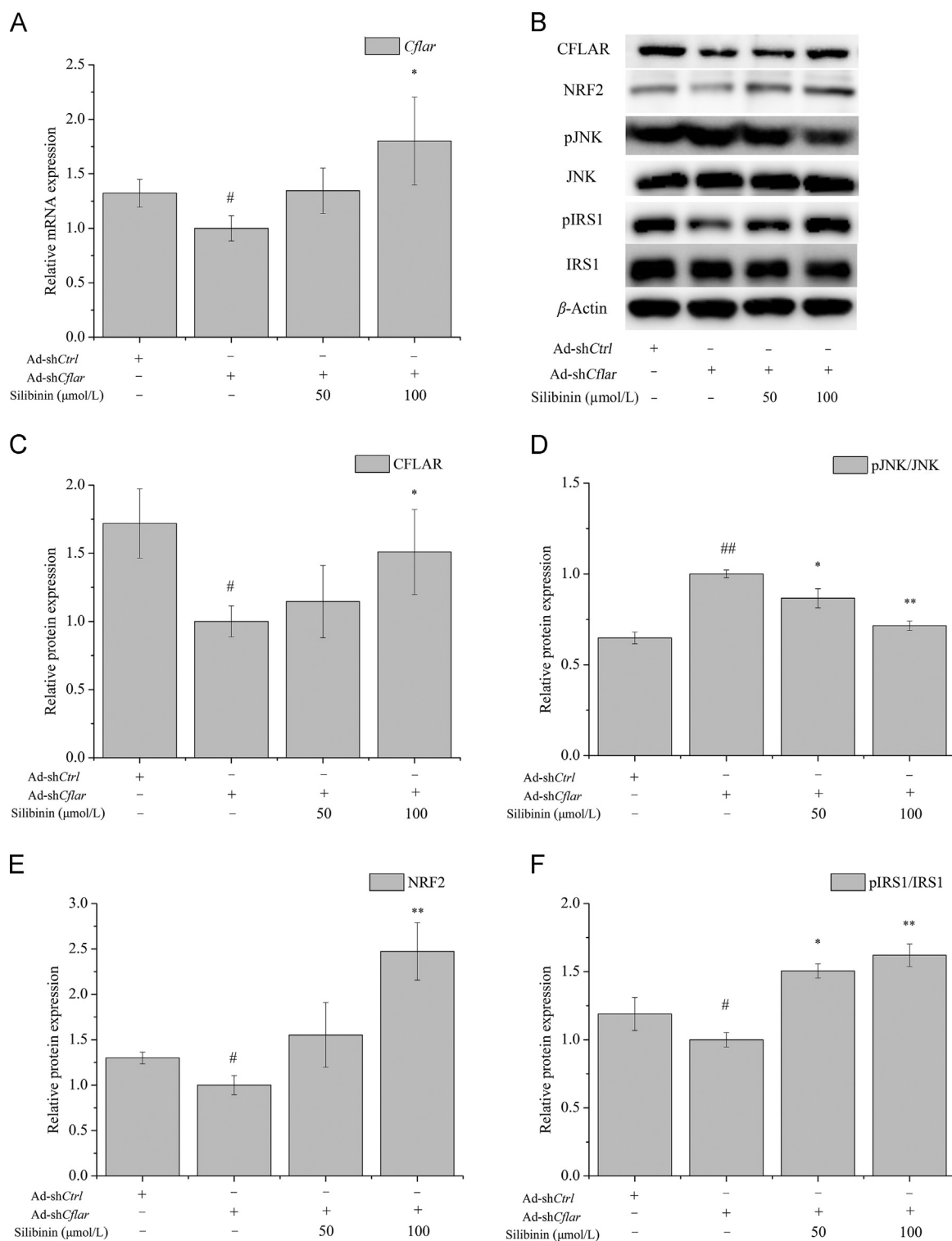


Figure 6 Effects of silibinin on the expression of CFLAR-JNK pathway-related genes in NCTC-1469 cells after adenovirus-mediated knock-down of *Cflar*. NCTC-1469 cells were transfected with adenovirus and then treated with silibinin to detect the cellular mRNA expression of *Cflar* (A), protein expression of CFLAR, pJNK/JNK, NRF2, and pIRS1/IRS1 (B)–(F). The representative results from three independent experiments were shown. Cellular protein expression levels were analyzed by Western blot. The relative protein levels were determined after normalization with β-actin. The data were expressed as the means ± SD. #*P* < 0.05 and ##*P* < 0.01 versus control group; **P* < 0.05 and ***P* < 0.01 versus model group. CFLAR, caspase 8 and Fas-associated protein with death domain-like apoptosis regulator; IRS1, insulin receptor substrate 1; JNK, c-Jun N-terminal kinase; NRF2, nuclear factor erythroid 2-related factor 2; pIRS1, phosphorylation of insulin receptor substrate 1; pJNK, phosphorylation of c-Jun N-terminal kinase.

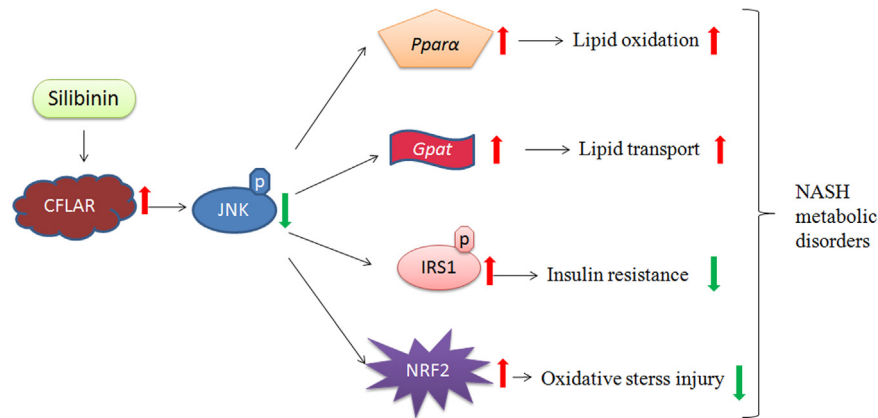


Figure 7 Proposed mechanism of silibinin against NASH. NASH, nonalcoholic steatohepatitis.

5. Conclusions

One important finding in this paper is the regulation of silibinin on NASH-related CFLAR-JNK pathway. Silibinin can prevent NASH by activating the expression of CFLAR and inhibiting the phosphorylation of JNK, thereby regulating NASH-related hepatic lipid metabolism, insulin resistance and oxidative stress. The other important finding in this paper is the regulation of silibinin on NASH-related NRF2 pathway. Silibinin also can up-regulate the expression of NRF2 and thereby modulate the activities of antioxidative and pro-oxidative enzymes to relieve hepatic oxidative stress injury. The proposed regulatory mechanism of silibinin against NASH was shown in Fig. 7.

Acknowledgments

This work was supported by Major Technological Innovation Project of Hubei Province (Grant no. 2016ACA140, China) and Innovation and Entrepreneurship Training Project for College Students of the Ministry of Education (Grant no. 201610512001, China).

References

- Kleiner DE, Brunt EM, van Natta M, Behling C, Contos MJ, Cummings OW, et al. Design and validation of a histological scoring system for nonalcoholic fatty liver disease. *Hepatology* 2005;**41**:313–21.
- Michelotti GA, Machado MV, Diehl AM. NAFLD, NASH and liver cancer. *Nat Rev Gastroenterol Hepatol* 2013;**10**:656–65.
- Byrne CD, Targher G. NAFLD: a multisystem disease. *J Hepatol* 2015;**62**:S47–64.
- Zhu Y, Liu H, Zhang M, Guo GL. Fatty liver diseases, bile acids, and FXR. *Acta Pharm Sin B* 2016;**6**:409–12.
- Nascimbeni F, Pais R, Bellentani S, Day CP, Ratziu V, Loria P, et al. From NAFLD in clinical practice to answers from guidelines. *J Hepatol* 2013;**59**:859–71.
- Labrecque DR, Abbas Z, Anania F, Ferenci P, Khan AG, Goh KL, et al. World Gastroenterology Organisation global guidelines: non-alcoholic fatty liver disease and nonalcoholic steatohepatitis. *J Clin Gastroenterol* 2014;**48**:467–73.
- Carazo A, León J, Casado J, Gila A, Delgado S, Martín A, et al. Hepatic expression of adiponectin receptors increases with non-alcoholic fatty liver disease progression in morbid obesity in correlation with glutathione peroxidase 1. *Obes Surg* 2011;**21**:492–500.
- Zhang HJ, He J, Pan LL, Ma ZM, Han CK, Chen CS, et al. Effects of moderate and vigorous exercise on nonalcoholic fatty liver disease: a randomized clinical trial. *JAMA Intern Med* 2016;**176**:1074–82.
- Boschbarrera J, Menendez JA. Silibinin and STAT3: a natural way of targeting transcription factors for cancer therapy. *Cancer Treat Rev* 2015;**41**:540–6.
- Muthumani M, Prabu SM. Silibinin potentially protects arsenic-induced oxidative hepatic dysfunction in rats. *Toxicol Mech Methods* 2012;**22**:277–88.
- Zhang Y, Hai J, Cao M, Zhang Y, Pei S, Wang J, et al. Silibinin ameliorates steatosis and insulin resistance during non-alcoholic fatty liver disease development partly through targeting IRS-1/PI3K/Akt pathway. *Int Immunopharmacol* 2013;**17**:714–20.
- Haddad Y, Vallerand D, Brault A, Haddad PS. Antioxidant and hepatoprotective effects of silibinin in a rat model of nonalcoholic steatohepatitis. *Evid Based Complement Alternat Med* 2011:nep164.
- Serviddio G, Bellanti F, Giudetti AM, Gnoni GV, Petrella A, Tamborra R, et al. A silybin-phospholipid complex prevents mitochondrial dysfunction in a rodent model of nonalcoholic steatohepatitis. *J Pharmacol Exp Ther* 2010;**332**:922–32.
- Loguercio C, Andreone P, Brisc C, Brisc MC, Bugianesi E, Chiaramonte M, et al. Silybin combined with phosphatidylcholine and vitamin E in patients with nonalcoholic fatty liver disease: a randomized controlled trial. *Free Radic Biol Med* 2012;**52**:1658–1665.
- Wang PX, Ji YX, Zhang XJ, Zhao LP, Yan ZZ, Zhang P, et al. Targeting CASP8 and FADD-like apoptosis regulator ameliorates nonalcoholic steatohepatitis in mice and nonhuman primates. *Nat Med* 2017;**23**:439–49.
- Cheng Y, Huang L, Ping J, Chen T, Chen J. MicroRNA-199a-3p attenuates hepatic lipogenesis by targeting Sp1. *Am J Transl Res* 2017;**9**:1905–13.
- Chen J, Liu J, Wang Y, Hu X, Zhou F, Hu Y, et al. Wogonin mitigates nonalcoholic fatty liver disease via enhancing PPAR α /AdipoR2, *in vivo* and *in vitro*. *Biomed Pharmacother* 2017;**91**:621–31.
- Zheng R, Dragomir AC, Mishin V, Richardson JR, Heck DE, Laskin DL, et al. Differential metabolism of 4-hydroxynonenal in liver, lung and brain of mice and rats. *Toxicol Appl Pharmacol* 2014;**279**:43–52.
- Liang J, Liu C, Qiao A, Cui Y, Zhang H, Cui A, et al. MicroRNA-29a-c decrease fasting blood glucose levels by negatively regulating hepatic gluconeogenesis. *J Hepatol* 2013;**58**:535–42.
- Flores-Costa R, Alcaraz-Quiles J, Titos E, López-Vicario C, Casulleras M, Duran-Güell M, et al. The soluble guanylate cyclase stimulator IW-1973 prevents inflammation and fibrosis in experimental non-alcoholic steatohepatitis. *Br J Pharmacol* 2017;**175**:953–67.
- Krawczyk M, Bonfrate L, Portincasa P. Nonalcoholic fatty liver disease. *Best Pract Res Clin Gastroenterol* 2010;**24**:695–708.
- Day CP, Saksena S. Non-alcoholic steatohepatitis: definitions and pathogenesis. *J Gastroenterol Hepatol* 2002;**17**:S377–84.
- Schattenberg JM, Zimmermann T, Wörms M, Sprinzl MF, Kreft A, Kohl T, et al. Ablation of c-FLIP in hepatocytes enhances death-receptor mediated apoptosis and toxic liver injury *in vivo*. *J Hepatol* 2011;**55**:1272–80.

24. Kohl T, Gehrke N, Schad A, Nagel M, Wörms MA, Sprinzl MF, et al. Diabetic liver injury from streptozotocin is regulated through the caspase-8 homolog cFLIP involving activation of JNK2 and intrahepatic immunocompetent cells. *Cell Death Dis* 2013;**4**:e712.
25. Schattenberg JM, Nagel M, Kim YO, Kohl T, Wörms MA, Zimmermann T, et al. Increased hepatic fibrosis and JNK2-dependent liver injury in mice exhibiting hepatocyte-specific deletion of cFLIP. *Am J Physiol Gastrointest Liver Physiol* 2012;**303**:G498–506.
26. Cong WN, Tao RY, Tian JY, Liu GT, Ye F. The establishment of a novel non-alcoholic steatohepatitis model accompanied with obesity and insulin resistance in mice. *Life Sci* 2008;**82**:983–90.
27. Seo YS, Kim JH, Jo NY, Choi KM, Baik SH, Park JJ, et al. PPAR agonists treatment is effective in a nonalcoholic fatty liver disease animal model by modulating fatty-acid metabolic enzymes. *J Gastroenterol Hepatol* 2008;**23**:102–9.
28. Forcheron F, Cachefo A, Thevenon S, Pinteur C, Beylot M. Mechanisms of the triglyceride- and cholesterol-lowering effect of fenofibrate in hyperlipidemic type 2 diabetic patients. *Diabetes* 2002;**51**:3486–91.
29. Wang C, Duan X, Sun X, Liu Z, Sun P, Yang X, et al. Protective effects of glycyrrhizic acid from edible botanical *Glycyrrhiza glabra* against non-alcoholic steatohepatitis in mice. *Food Funct* 2016;**7**:3716–23.
30. Furuhashi M, Hotamisligil GS. Fatty acid-binding proteins: role in metabolic diseases and potential as drug targets. *Nat Rev Drug Discov* 2008;**7**:489–503.
31. Ntambi JM, Miyazaki M. Regulation of stearoyl-CoA desaturases and role in metabolism. *Prog Lipid Res* 2004;**43**:91–104.
32. Cao J, Li JL, Li D, Tobin JF, Gimeno RE. Molecular identification of microsomal acyl-CoA:glycerol-3-phosphate acyltransferase, a key enzyme in *de novo* triacylglycerol synthesis. *Proc Natl Acad Sci U S A* 2006;**103**:19695–700.
33. Lettéron P, Sutton A, Mansouri A, Fromenty B, Pessayre D. Inhibition of microsomal triglyceride transfer protein: another mechanism for drug-induced steatosis in mice. *Hepatology* 2003;**38**:133–40.
34. Rizki G, Arnaboldi L, Gabrielli B, Yan J, Lee GS, Ng RK, et al. Mice fed a lipogenic methionine-choline-deficient diet develop hypermetabolism coincident with hepatic suppression of SCD-1. *J Lipid Res* 2006;**47**:2280–90.
35. Chang X, Yan H, Fei J, Jiang M, Zhu H, Lu D, et al. Berberine reduces methylation of the MTTP promoter and alleviates fatty liver induced by a high-fat diet in rats. *J Lipid Res* 2010;**51**:2504–15.
36. Zhang B, Xue C, Hu X, Xu J, Li Z, Wang J, et al. Dietary sea cucumber cerebroside alleviates orotic acid-induced excess hepatic adipogenesis in rats. *Lipids Health Dis* 2012;**11**:48.
37. Wetterau JR, Aggerbeck LP, Bouma ME, Eisenberg C, Munck A, Hermier M, et al. Absence of microsomal triglyceride transfer protein in individuals with abetalipoproteinemia. *Science* 1992;**258**:999–1001.
38. Kawano Y, Cohen DE. Mechanisms of hepatic triglyceride accumulation in non-alcoholic fatty liver disease. *J Gastroenterol* 2013;**48**:434–41.
39. Rinella ME. Nonalcoholic fatty liver disease: a systematic review. *J Am Med Assoc* 2015;**313**:2263–73.
40. Chen X, Zhao X, Lan F, Zhou T, Cai H, Sun H, et al. Hydrogen sulphide treatment increases insulin sensitivity and improves oxidant metabolism through the CaMKK β -AMPK pathway in PA-induced IR C2C12 cells. *Sci Rep* 2017;**7**:13248.
41. Li G, Luan G, He Y, Tie F, Wang Z, Suo Y, et al. Polyphenol stilbenes from fenugreek (*Trigonella foenum-graecum* L.) seeds improve insulin sensitivity and mitochondrial function in 3T3-L1 adipocytes. *Oxid Med Cell Longev* 2018;**2018**:7634362.
42. Zhu Q, Zhu R, Jin J. Neutral ceramidase-enriched exosomes prevent palmitic acid-induced insulin resistance in H4IIEC3 hepatocytes. *FEBS Open Bio* 2016;**6**:1078–84.
43. Aguirre V, Werner ED, Giraud J, Lee YH, Shoelson SE, White MF. Phosphorylation of Ser307 in insulin receptor substrate-1 blocks interactions with the insulin receptor and inhibits insulin action. *J Biol Chem* 2002;**277**:1531–7.
44. Yesilova Z, Yaman H, Oktenli C, Ozcan A, Uygun A, Cakir E, et al. Systemic markers of lipid peroxidation and antioxidants in patients with nonalcoholic fatty liver disease. *Am J Gastroenterol* 2005;**100**:850–5.
45. Vomund S, Schäfer A, Parnham MJ, Brüne B, von Knethen A. Nrf2, the master regulator of anti-oxidative responses. *Int J Mol Sci* 2017;**18**: pii: E2772.
46. Lee SY, Chen PY, Lin JC, Kirkby NS, Ou CH, Chang TC. Melaleuca alternifolia induces heme oxygenase-1 expression in murine RAW264.7 cells through activation of the Nrf2-ARE pathway. *Am J Chin Med* 2017;**45**:1631–48.
47. Yin J, Ma L, Wang H, Yan H, Hu J, Jiang W, et al. Chinese herbal medicine compound Yi-Zhi-Hao pellet inhibits replication of influenza virus infection through activation of heme oxygenase-1. *Acta Pharm Sin B* 2017;**7**:630–7.
48. Zeng X, Li X, Xu C, Jiang F, Mo Y, Fan X, et al. *Schisandra sphenanthera* extract protects against chronic-binge and acute alcohol-induced liver injury by regulating the NRF2-ARE pathway in mice. *Acta Pharm Sin B* 2017;**7**:583–92.
49. Park JS, Shim YJ, Kang BH, Lee WK, Min BH. Hepatocyte-specific clusterin overexpression attenuates diet-induced nonalcoholic steatohepatitis. *Biochem Biophys Res Commun* 2018;**495**:1775–81.
50. Rezaazadeh A, Yazdanparast R, Molaei M. Amelioration of diet-induced nonalcoholic steatohepatitis in rats by Mn–salen complexes via reduction of oxidative stress. *J Biomed Sci* 2012;**19**:26.
51. Tariq Z, Green CJ, Hodson L. Are oxidative stress mechanisms the common denominator in the progression from hepatic steatosis towards non-alcoholic steatohepatitis (NASH)? *Liver Int* 2014;**34**: e180–90.
52. Leclercq IA, Farrell GC, Field J, Bell DR, Gonzalez FJ, Robertson GR. CYP2E1 and CYP4A as microsomal catalysts of lipid peroxides in murine nonalcoholic steatohepatitis. *J Clin Invest* 2000;**105**:1067–75.
53. Weltman MD, Farrell GC, Liddle C. Increased hepatocyte CYP2E1 expression in a rat nutritional model of hepatic steatosis with inflammation. *Gastroenterology* 1996;**111**:1645–53.
54. Weltman MD, Farrell GC, Hall P, Ingelman-Sundberg M, Liddle C. Hepatic cytochrome P450 2E1 is increased in patients with nonalcoholic steatohepatitis. *Hepatology* 1998;**27**:128–33.
55. Abdelmegeed MA, Banerjee A, Yoo SH, Jang S, Gonzalez FJ, Song BJ. Critical role of cytochrome P450 2E1 (CYP2E1) in the development of high fat-induced nonalcoholic steatohepatitis. *J Hepatol* 2012;**57**:860–6.